Technical Sciences 17(4), 2014, 321–335

DARCY'S AND FORCHHEIMER'S LAWS IN PRACTICE. PART 1. THE EXPERIMENT

***Wojciech Sobieski*[1], *Anna Trykozko*[2]**

[1] Department of Mechanics and Machine Design
University of Warmia and Mazury in Olsztyn
[2] Interdisciplinary Centre for Mathematical and Computational Modeling
University of Warsaw

Received 3 April 2014, accepted 8 November 2014, available on line 11 November 2014.

K e y w o r d s: Darcy's law, Forchheimer's law, Forchheimer Plot Method, porous media, permeability.

A b s t r a c t

The aim of this study is to derive flow parameters, which are permeability and Forchheimer coefficient, based on experimentally measured flow rates and pressure drops. When flow rates used in measurements exceed the limits of linear Darcy's flow regime we discuss what needs to be taken into account while processing the measurements. The study consists of two parts. In this part we briefly recall Darcy's and Forchheimer's laws and address the issue of detecting transition between ranges of their applicability. Then we describe the experiment and discuss 8 different ways to process measurement data, four for Darcy's, and four for Forchheimer's models. The main topic of the second part is to provide recommendations for the best ways to process data, so that the results obtained with numerical models are in the best agreement with the experimental data. The results shown in the two papers belong to a larger work devoted to modeling fluid flows through porous media, with a special interest in granular beds.

Introduction

A fundamental law linking pressure drop and velocity in fluid flow through porous media is Darcy's law (1856). It can be applied to flows of gases, liquids, or mixtures. Darcy's law may be written as follow (BEAR 1972, CATALANO 2012, HELLSTRÖM, LUNDSTRÖM 2006):

$$-\frac{\mathrm{d}p}{\mathrm{d}x} = \frac{1}{\kappa} \cdot (\mu \cdot \vec{v_f}) \tag{1}$$

Correspondence: Wojciech Sobieski, Katedra Mechaniki i Podstaw Konstrukcji Maszyn, Uniwersytet Warmińsko-Mazurski, ul. M. Oczapowskiego 11, 10-957 Olsztyn, phone: +48 89 523 32 40, e-mail: wojciech.sobieski@uwm.edu.pl

where:
p – pressure [Pa],
x – coordinate [m],
κ – permeability coefficient [m^2],
μ – dynamic viscosity coefficient of the fluid [kg/(m · s)],
$\vec{v}_f$ – filtration velocity [m/s].

For low flow velocities, Darcy's law correctly describes the flow in porous media (HELLSTRÖM, LUNDSTRÖM 2006). However, as velocities become larger, a discrepancy between experimental data and results obtained for Darcy's law appears. FORCHHEIMER (1901) linked this discrepancy to inertial effects and suggested to add to (1) a term representing kinetic energy (ANDRADE et al. 1999, BEAR 1972, EWING et al. 1999, HELLSTRÖM, LUNDSTRÖM 2006):

$$-\frac{\mathrm{d}p}{\mathrm{d}x} = \frac{1}{\kappa} \cdot (\mu \cdot \vec{v}_f) + \beta \cdot (\rho \cdot \vec{v}_f^{\,2}) \tag{2}$$

where:
β – Forchheimer coefficient (also known as non-Darcy coefficient, or β factor) [1/m],
ρ – density of the fluid [kg/m^3].

It is common to define limits of the Darcy's law validity by means of Reynolds number Re [-], defined as

$$\mathrm{Re} = \frac{\rho \cdot |\vec{v}_f| \cdot d}{\mu} \tag{3}$$

where:
d – the average particle diameter [m].

Most often it is assumed that the upper limit of the applicability of Darcy's law is between Re = 1 and Re = 10 (BEAR 1972, CHAPMAN 1981, HASSANIZADEH, GRAY 1987, SUKOP et al. 2013, TINDALL et al. 1988). Other works indicate the upper limit of Darcy's law as Re = 1 (ALABI 2011), Re = 2 (HASSANIZADEH, GRAY 1987), Re = 3 (HASSANIZADEH, GRAY 1987) or Re = 5 (HASSANIZADEH, GRAY 1987, SAWICKI et al. 2004). Some authors suggest that the upper limit goes above Re = 10 (CHAPMAN 1981, HASSANIZADEH, GRAY 1987). This ambiguity raises a question about which model is appropriate in cases where a range of velocities under consideration probably goes beyond the Darcy's flow regime. In the current work we address this question.

Both laws (1) and (2) are well known and can be found in many textbooks and papers. The available literature provides many general formulas to calculate permeability and Forchheimer coefficients based on such parameters of porous media as porosity or tortuosity (HUANG, AYOUB 2008), but the formulas are usually empirical and not universal. As we have shown in (SOBIESKI, TRYKOZKO 2001), different formulas computed with a fixed set of parameters can lead to totally different values of β coefficients, ranging even over several orders of magnitude.

The problem of assigning appropriate models and coefficients raises a question of a strategy to choose while processing experimental data. It is important for practical purposes of real systems design, as well as to create and verify mathematical models.

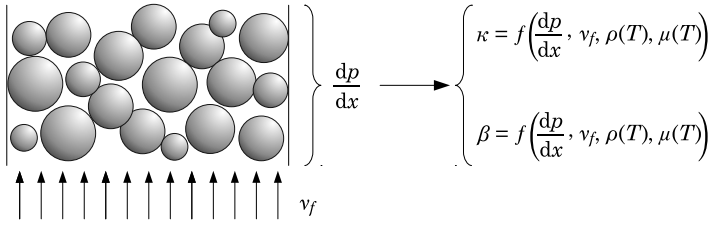

Fig. 1. The scheme of inverse problem

In the current work we suggest that in order to obtain all needed coefficients, an inverse problem using a test porous bed should be solved (Fig. 1). Thus obtained values may be used in other systems with the same porous medium and similar ranges of Reynolds numbers as well as in other investigations. Though the approach seems to be quite straightforward, there are several questions to be answered:

– How to prepare an experiment that will provide the best quality of results?

– In which way should the experimental data be analyzed?

– How to proceed in the case when the range of Reynolds numbers covered by the experiment spans over the Darcy's and Forchheimer flow regimes?

An attempt to discuss the above issues constitutes the main objectives of this study and is given mainly in the second part of the work. The current part contains details on preparing and collecting experimental data. The conclusions are based on the methodology developed in (SOBIESKI 2010), in which as the best experimental data we consider the data that gives the best agreement between numerical model (or the theory) and the experiment over the whole range of basic parameters.

It should be mentioned that a recent growth in available computer power has given rise to another approach, which we call a virtual experiment. Instead of a physical experiment, numerical simulations of flow at pore scale are performed by solving Navier-Stokes equations. Thanks to microimaging techniques it is feasible to consider flows in geometries reflecting realistic pore structures. By upscaling pore-scale solutions to the continuum core scale it is possible to study the models, parameters and appropriate relationships, see (PESZYŃSKA, TRYKOZKO 2013) and references therein.

Experimental study

A sketch of equipment used in experimental investigations is given in Figure 2. It consists of a plexiglass pipe filled with granulate (6), recharged from the bottom, with water coming from a container (1) through a pump (2). Intensity of flow is controlled by a valve (3). After passing through a bed, water reaches the upper reservoir (7), and then, through the overfall (8) goes down to the bottom reservoir. The flow intensity is measured by a rotameter (5). Piezometric heads

$$h = \frac{p}{\rho \cdot g} + z \tag{4}$$

where g is the gravity acceleration [m/s^2] and is a fixed reference level [m], are measured by means of U-tube manometers linked to connector pipes (10). Water temperature is measured by thermometer (9). Errors of measurement were as follows: flow intensity 0.000000056 [m^3/s]; piezometric head 1.0 [mm H_2O]; temperature 0.1 [K]. A glass bead pack was used as the porous medium. Main parameters are summarized in Tabela 1.

During the experiment, 10 measurements were made for each of 12 different values of volumetric flow Q^V. For a given volumetric flow, the resulting water levels (measured from a reference level) at four points along the measurement pipe were taken. The measurement points were equally distributed along the column with a distance 0.3 [m]. Based on these values and the column cross-section S, mean filtration velocity $\vec{v}_f$, pressure differences Δp between measurements points as well as Reynolds numbers were computed for every flow rate. In order to unify data and facilitate comparison with results of numerical simulation, pressures were related to the highest measurement point (Fig. 2, point 1). Results of measurements are summarized in Tabela 2.

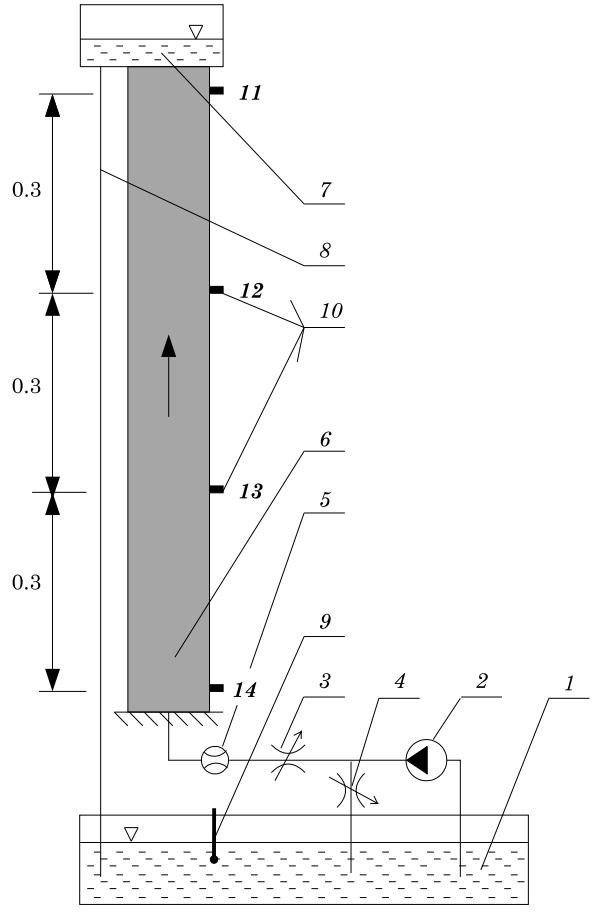

1 – bottom reservoir, *2* – pump, *3* – valve, *4* – overfall valve,
5 – rotameter, *6* – porous bed, *7* – upper reservoir,
8 – valve, *9* – thermometer, *10* – stub pipe,
11–14 – measurement points

Fig. 2. Scheme of the laboratory stand

A relationship between pressure drop and flow velocity imposed at the inlet is the basic relationship: its plot is given in Figure 3. Values obtained for pressure drop measured between extreme measurement points (thus, along the whole length of the column) are plotted with a solid line. Dashed lines mark minimum and maximum values of pressure drops measured for a given inlet velocity by applying different configurations of measurement sections. The relationship is non-linear, what suggests that the mesurements cover the region of the Fochheimer law's validity.

Increasing the length of the measurement section causes the global error of measurements to decrease. For this reason, in all computations that follow,

Table 1

Parameters of the experiment

Parameter	Symbol	Value
Average water temperature	T	306.63 [K]
Density of water	ρ	994.49 [kg/m^3]
Dynamic viscosity coefficient	μ	0.000742784 [kg/(m · s)]
Kinematic viscosity coefficient	ν	0.000000747 [m^2/s]
Area of a porous bed cross-section	S	0.005 [m^2]
Distance between measurement points 1–4	L	0.9 [m]
Porosity coefficient of granulate	e	0.37 [-]
Solid fraction	ε	0.63 [-]
Average diameter of glass beads	d	1.95 [mm]
Gravity acceleration	g	9.81 [m/s^2]

Table 2

Results of measurements

Q^V	h_1	h_2	h_3	h_4	$\vec{v}_f$	Δp_{4-1}	Δp_{3-1}	Δp_{2-1}	Re
$\cdot 10^{-3}$ [m^3/s]	[mm H_2O]	[mm H_2O]	[mm H_2O]	[mm H_2O]	$\cdot 10^{-3}$ [m/s]	[Pa]	[Pa]	[Pa]	[-]
5.66	357.50	362.20	365.90	370.60	0.313	127.80	81.95	45.85	0.82
22.09	**358.00**	**374.90**	**387.60**	**402.70**	**1.221**	**436.09**	**288.78**	**164.88**	**3.19**
38.52	**359.50**	**388.90**	**411.70**	**440.10**	**2.129**	**786.33**	**509.26**	**286.82**	**5.56**
54.95	**360.90**	**403.30**	**438.10**	**478.80**	**3.037**	**1150.22**	**753.16**	**413.65**	**7.93**
71.38	**362.80**	**419.20**	**466.60**	**520.50**	**3.945**	**1538.51**	**1012.67**	**550.23**	**10.30**
87.81	365.20	436.60	496.20	564.70	4.853	1946.31	1278.03	696.57	12.67
104.24	367.00	453.50	527.40	610.80	5.761	2378.50	1564.85	843.89	15.04
120.67	368.90	471.80	559.90	660.30	6.669	2842.88	1863.38	1003.89	17.41
137.11	371.40	492.10	598.00	716.50	7.577	3366.77	2210.70	1177.54	19.78
153.54	374.20	516.40	641.50	779.70	8.485	3956.03	2607.76	1387.29	22.15
169.97	376.60	541.80	685.70	845.70	9.393	4576.51	3015.56	1611.68	24.52
182.29	378.90	562.20	721.90	901.80	10.074	5101.38	3346.29	1788.26	26.30

pressure drops always refer to the longest section L. The pressure drop may be calculated directly between points 1 and 4, or indirectly, using an approximation method taking into account pressure drops between sections 3–1, 4–2, 3–2, 4–3 and 2–1 as well.

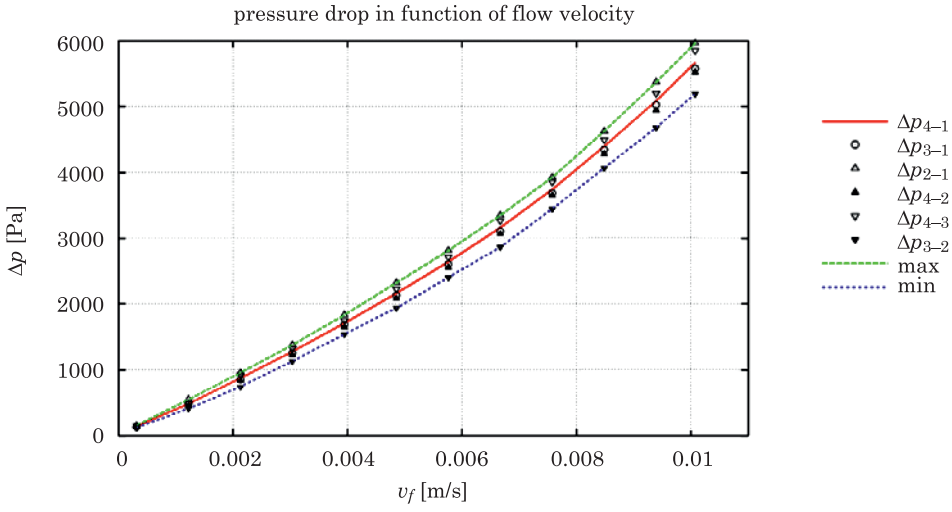

Fig. 3. Pressure drops measured between different pairs of measurement points

Figure 4 gives a plot of the effective permeability coefficient κ_{eff} as a function of velocity, computed following the formula:

$$\kappa_{eff} = \frac{\mu \cdot |\vec{v}_f|}{\frac{\mathrm{d}p}{\mathrm{d}x}} \tag{5}$$

A notion of 'effective' is used in order to emphasize that κ_{eff} in (5) is equivalent to the permeability coefficient κ in (1) only within the ranges of validity of Darcy's law. In general, coefficient κ_{eff} of (5) represents not only the permeability coefficient κ characterizing the medium, but also inertial effects. Effective permeability decreases with increasing flow velocities due to growing inertial effects. It is visible after rewriting the Forchheimer law (2) in the form:

$$-\frac{\mathrm{d}p}{\mathrm{d}x} = \left(\frac{1}{\kappa} + \frac{\beta \cdot \rho \cdot \vec{v}_f}{\mu}\right) \cdot \mu \cdot \vec{v}_f = \frac{\mu}{\kappa_{eff}} \cdot \vec{v}_f \tag{6}$$

It can be seen that the first point in Figure 4 differs from the others. The flow intensity in this case was very close to the lower limit of the measurement range of the rotameter. Since we doubt about reliability of this measurement, we decided not to take it into account in further investigations.

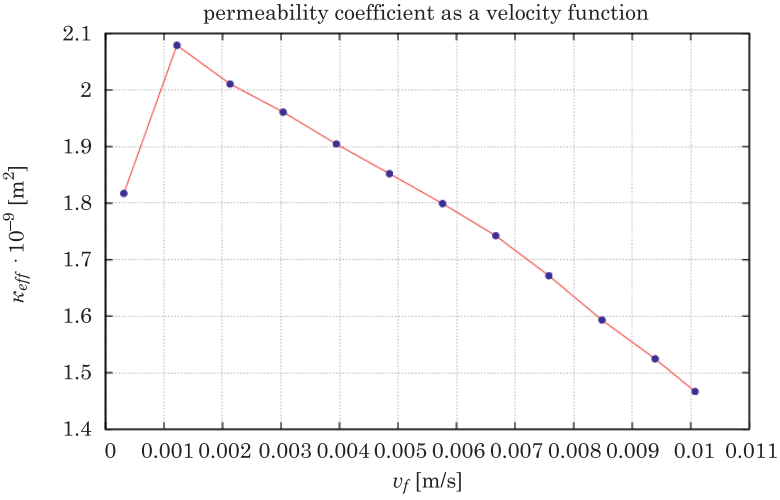

Fig. 4. Effective permeability coefficient as a function of velocity

Due to the rotameter characteristics we have not got enough data belonging to the linear flow regime what would be manifested by a constant ratio of flow rates and pressure drops. Thus the range of flow rates covered by the measurements does not allow to capture the onset of inertia effects. On the other hand, the Reynolds values less or close to 10 (Tab. 2) allow to consider flow cases 2–5 as belonging to the transition zone between the linear and nonlinear flow regimes. Therefore in what follows we consider the cases 2–5 as an approximation of the linear flow regime. Figure 5 shows the pressure drop calculated for the average value of the effective permeability coefficient according to Darcy's law. The averaging was performed two times: for cases 2–12 (the whole range of Reynolds numbers), and for flow cases 2–5. As expected, the linear model does not apply to the whole range of velocities. The discrepancy grows when the filtration velocities increase. This result shows why we consider the two cases: case 2–5 and case 2–12 separately.

After analyzing the measurement data and taking into account the range of Darcy's law validity we summarize that:

– The first point in Figure 4 will be not taken into account in further investigations due to the possibility of large flow measurement errors.

– All remaining values suggest presence of additional resistance forces in flow.

– We consider the flow case 5 as the last one to belong to the range of application of Darcy's law. The Reynolds number value for this measurement is close to the transition limit the most often suggested in the literature (Re $\approx$ 10). A distinction between the ranges of validity of Darcy's and

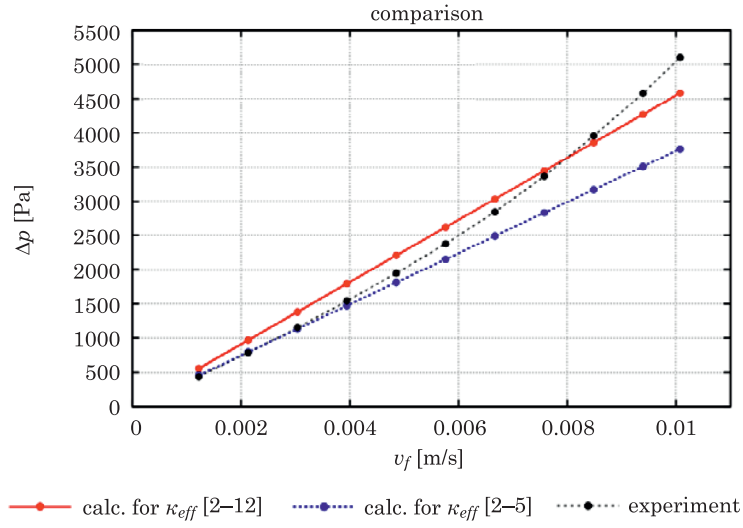

Fig. 5. Pressure drops as a function of velocity

Forchheimer's laws is necessary in order to perform further computations; this point will be discussed later.

– On the other hand, the transition between linear and non-linear regimes is smooth, therefore we are aware that this decision is somewhat arbitrary.

– The maximal Reynolds number reached during experiments does not exceed 30, and is thus several times smaller than the value considered to be the upper limit of validity of the Forchheimer law (HUANG, AYOUB 2008).

Computation of porous media parameter – linear model

The permeability coefficient κ is the main parameter characterizing porous media in a linear model. Four different methods were applied in order to compute this coefficient. Only results for measurements 2–5, with less or close to, were taken into account.

The first method followed directly Darcy's law (1) rewritten in the form:

$$\kappa = \mu \cdot \vec{v}_f \cdot \frac{L}{\Delta p} \tag{7}$$

where pressure drop along a segment $\Delta p/L$ replaces a more general notion of $\mathrm{d}p/\mathrm{d}x$.

Given measured piezometric heads h, differences Δp in pressures between the highest and the lowest measurement points were computed, to finally get the permeability coefficient κ. We also report values of the hydraulic conductivity coefficient K[m/s]

$$K = \kappa \cdot \frac{\rho \cdot g}{\mu} \tag{8}$$

which is commonly used in hydrogeology. As a last step, values of coefficients obtained for the same inlet velocities were averaged. Results are given in Table 3.

Table 3

Permeability coefficient calculations – method 1

$\vec{v_f} \cdot 10^{-3}$ [m/s]	Δh_{4-1} [m]	Δp_{4-1} [Pa/m]	K [m/s]	κ [m^2]
1.221	0.0447	484.545	0.02458	1.871E-009
2.129	0.0806	873.698	0.02377	1.8010E-009
3.037	0.1179	1278.028	0.02318	1.765E-009
3.945	0.1577	1709.457	0.02251	1.714E-009
–	–	–	0.02351	1.790E-009

The second method differed in the way that differences in piezometric heads Δh_{4-1} between measurement points 4 and 1 were computed. Since method 1 does not take into account measurements obtained for inner points 2 and 3, this time for each velocity inlet a linear function approximating piezometric heads was found. Differences Δh_{4-1} were computed based not on measured data, but on approximated values. Results are summarized in Table 4.

Table 4

Permeability coefficient calculations – method 2

$\vec{v_f} \cdot 10^{-3}$ [m/s]	Δh_{4-1} [m]	Δp_{4-1} [Pa/m]	K [m/s]	κ [m^2]
1.221	0.0440	429.651	0.024946	1.899E-009
2.129	0.0794	774.426	0.024135	1.838E-009
3.037	0.1165	1137.054	0.023449	1.785E-009
3.945	0.1561	1523.390	0.022736	1.731E-009
–	–	–	0.023816	1.813E-009

In methods 3 and 4 values of Δh_{4-1} are computed as in method 1 (Table 3). The pressure drops as a function of velocities are approximated with a linear function, its coefficient being equal to permeability. In method 3 no constraints

on a free-term were assigned, whereas method 4 assumed that the approximation line should pass through the origin of the coordinate system (free term equals zero). Results are given in Tabela 5.

Table 5

Permeability coefficient calculations – methods 3 and 4

Method	K [m/s]	κ [m^2]
Method 3:	0.02172	1.653E-09
Method 4:	0.02298	1.750E-09

If the permeability coefficient is known, the pressure drop between points 4 and 1 may be calculated according to (1). The impact of the method of data analysis is visualized in Figure 6. Errors due to methods 1 through 4 will be quantified in Part 2.

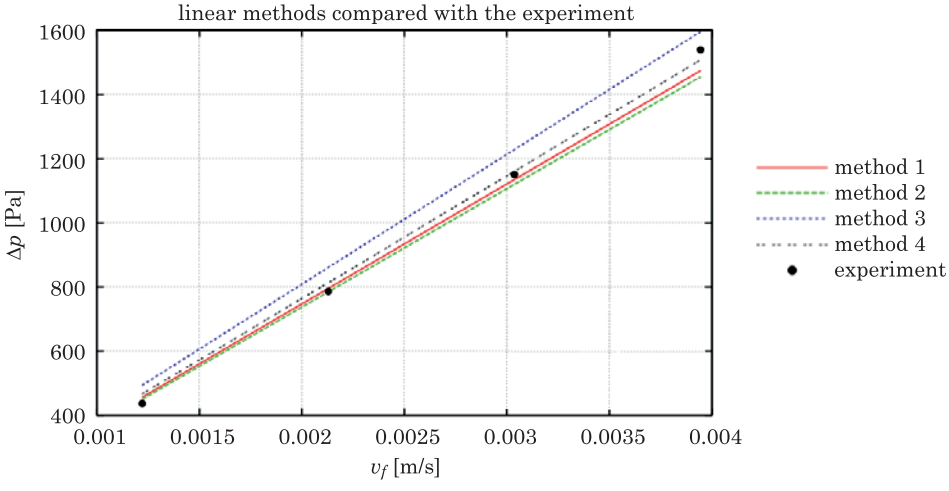

Fig. 6. Impact of data analysis on the agreement with the experiment for linear methods

Computation of porous media parameters – nonlinear model

In order to compute parameters κ and β based on experimental data, the Forchheimer Plot Method is used (HUANG, AYOUB 2008, ORODU et al. 2012, VAN BATENBURG, MILTON-TAYLER 2005). To this aim, the Forchheimer equation is rearranged to the form:

$$-\frac{\mathrm{d}p}{\mathrm{d}x}\cdot\frac{1}{\vec{v}_f\cdot\mu}=\frac{1}{\kappa}+\beta\left(\frac{\rho\cdot\vec{v}_f}{\mu}\right) \tag{9}$$

By introducing new variables:

$$\begin{cases} Y=-\dfrac{\mathrm{d}p}{\mathrm{d}x}\cdot\dfrac{1}{\vec{v}_f\cdot\mu} \\ X=\dfrac{\rho\cdot\vec{v}_f}{\mu} \end{cases} \tag{10}$$

a linear relationship is obtained:

$$Y=\beta\cdot X+\frac{1}{\kappa} \tag{11}$$

Measurement data were transformed following (10) and then parameters of a linear function (11) we are computed with the least-squares approximation. Two cases were distinguished. In Model A only data obtained for 6–12 measurement points (non-Darcy flows) were considered, whereas in model B also data obtained for slower flows (2–12) were taken into account (Fig. 7).

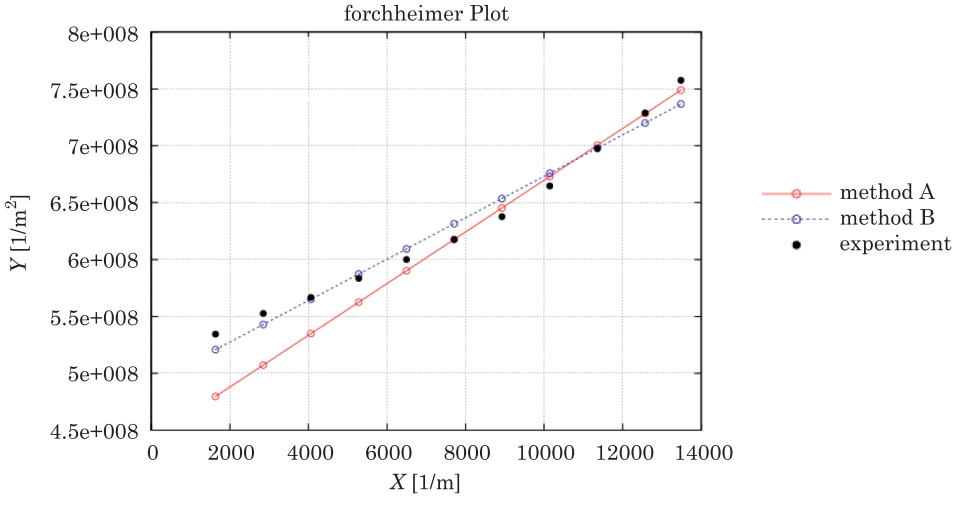

Fig. 7. Relationship between terms X and Y

An alternative way of computing parameters κ and β used original measurement data and was based on a least-square approximation with a quadratic function and a free term assumed to be zero. Again, two cases were

distinguished: Model C – based on non-Darcy flow data 6–12 only, and Model D, based on measurements 2–12. A summary of the computed parameters is given in Tabela 6. A comparison of non-linear methods and the experiment is shown in the Figure 8.

Table 6

Parameters κ and β computed with different methods

Method	K [m/s]	κ [m^2]	β [1/m]
Method A	0.02968	2.260E-09	22721.53
Method B	0.02675	2.037E-09	18215.36
Method C	0.03056	2.327E-09	23886.79
Method D	0.02874	2.188E-09	21569.43

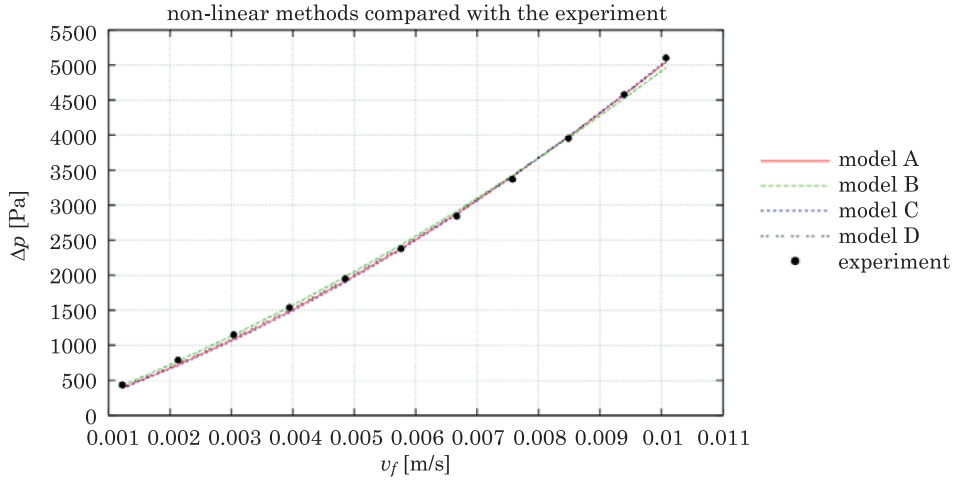

Fig. 8. Impact of data analysis on the agreement with the experiment for non-linear methods

Summary and conclusions

The range of flow rates covered by the experiment does not allow to precisely capture the onset of inertia effects. We have not got enough data belonging to the linear flow regime, what would be manifested by a constant ratio of flow rates and pressure drops. The rotameter characteristics did not let us to perform reliable experiments for lower flow rates. On the other hand, an attempt to make use of a graduated cylinder and a stop watch has proved not satisfactory, mostly due to instabilities in pressure drops observed during mesurements.

Thus the general conclusion is that in order to get a wider set of experimental data, an essentially different experimental set-up should be used. These will be a subject of our future works.

Due to practical difficulties mentioned above, we assumed here that the upper boundary of application of the Darcy law should be slightly above Re = 10. In this way we consider the flow cases from 2 to 5 (see Table. 1) to belong to the linear flow regime. This assumption does not introduce too much error, what is confirmed by the error analysis presented in the second part of the work.

As far as practical aspects of conducting measurements are concerned, the following remarks should be taken into account:

– The most important parameters are flow rates and pressure drops. Both should be measured with the highest available accuracy.

– In order to obtain higher quality of the data, every flow case (the same filtration velocity) should be repeated several times and then averaged (10 times seems to be enough, which is confirmed in Part 2 by small values of errors).

– The pressure drop should be measured over large sections of a sample. This would reduce the global error. The shorter measurement sections were, the higher was a difference between results and a line indicating the average (Fig. 3). However, in case of a nonhomogeneous layered packs, multiple mesurement points could be used to study local variations in pressure drops and to conclude about premeability variations.

– It is very important to keep the temperature constant during the experiment. This parameter does not appear explicitly in Darcy's, as well as Forchheimer law, but affects density and viscosity of the fluid. This conclusion was a result of our earlier investigations (SOBIESKI, TRYKOZKO 2011).

It is not possible to conclude which of the ways of data processing is the best for the mathematical model, which is shown in the Part 2. Our conclusions will be based on computations using numerical models and error analysis.

References

ALABI O.O. 2011. *Validity of Darcy's Law in Laminar Regime*. The Electronic Journal of Geotechnical Engineering, 16: 27–40.

ANDRADE J.S., COSTA U.M.S., ALMEIDA M.P., MAKSE H.A., STANLEY H.E. 1999. *Inertial Effects on Fluid Flow through Disordered Porous Media*. Physical Review Letters, 82(26): 5249–5252.

BATENBURG D. VAN, MILTON-TAYLER D. 2005. *Discussion on SPE 89325, Beyond beta factors: a complete model for Darcy, Forchheimer, and trans-Forchheimer flow in porous media*. JPT, 57(8): 72–73.

BEAR J. 1972. *Dynamics of Fluids in Porous Media*. Dover, New York.

CATALANO E. 2012. *A pore-scale coupled hydromechanical model for biphasos granular media*. PhD Thesis. University of Grenoble, France.

CHAPMAN R.E. 1981. *Geology and Water – An introduction to fluid mechanics for geologists*. Martinus Nijhoff & Dr. W. Junk Publishers, The Hague & Boston & London.

EWING R., LAZAROV R., LYONS S.L., PAPAVASSILIOU D.V., PASCIAK J., QIN G.X. 1999. *Numerical Well Model For Non-Darcy Flow*. Computational Geosciences, 3(3–4): 185–204.

HASSANIZADEH S.M., GRAY W.G. 1987. *High Velocity Flow in Porous Media*. Transport in Porous Media, 2(6): 521–531.

HELLSTRÖM J.G.I., LUNDSTRÖM T.S. 2006. *Flow through Porous Media at Moderate Reynolds Number*. 4th International Scientific Colloquium: Modelling for Material Processing. University of Latvia, Riga, Latvia, June 8–9.

HUANG H., AYOUB J. 2008. *Applicability of the Forchheimer Equation for Non-Darcy Flow in Porous Media*. SPE Journal, 13(1): 112–122.

ORODU O.D., MAKINDE F.A., ORODU K.B. 2012. *Experimental Study of Darcy and Non-Darcy Flow in Porous Media*. International Journal of Engineering and Technology, 2(12): 1934–1943.

PESZYŃSKA M., TRYKOZKO A. 2013. *Pore-to-core simulations of flow with large velocities using continuum models and imaging data*. Computational Geosciences, 17(4): 623–645.

SAWICKI J., SZPAKOWSKI W., WEINEROWSKA K., WOŁOSZYN E., ZIMA P. 2004. *Laboratory of Fluid Mechanics and Hydraulics*. Technical University of Gdańsk Publisher, Gdańsk, Poland (in Polish).

SOBIESKI W. 2010. *Use of Numerical Models in Validating Experimental Results*. Journal of Applied Computer Science, 18(1): 49–60.

SOBIESKI W., TRYKOZKO A. 2011. *Sensitivity aspects of Forchheimer's approximation*. Transport in Porous Media, 89(2): 155–164.

SUKOP M.C., HUANG H., ALVAREZ P.F., VARIANO E.A., CUNNINGHAM K.J. 2013. *Evaluation of permeability and non-Darcy flow in vuggy macroporous limestone aquifer samples with lattice Boltzmann methods*. Water Resources Research, 49(1): 1–15.

TINDALL J.A., KUNKEL J.R., ANDERSON D.E. 1998. *Unsaturated Zone Hydrology for Scientist and Engineers*. Pearson Education, New Jersey.